

Estimation of Lunar FeO and TiO₂ with Support Vector Regression Analysis and Evaluation of the Stokes Parameter Using M3 and LRO Mini RF Data.

Ajith Kumar Padinharethodi ¹, Shashi Kumar ², Advait CA ²

¹Al Sobaki General Maintenance Co LLC, Al Ain UAE- ajithpadinharethodi@gmail.com.

² Photogrammetry & Remote Sensing Department, Remote Sensing and Geoinformatics Group, Indian Institute of Remote Sensing, Indian Space Research Organisation, Dehradun, India, Pin: 248001- shashi@iirs.gov.in

² Photogrammetry & Remote Sensing Department, Remote Sensing and Geoinformatics Group, Indian Institute of Remote Sensing, Indian Space Research Organisation, Dehradun, India, Pin: 248001- advait.ca@iirsddn.ac.in

Key words: Moon Mineralogy Mapper (M3), LRO Mini RF SAR, Support vector Regression (SVR), Composite chemical content, Stokes parameter

Abstract

Moon Mineralogy Mapper (M3), the hyperspectral sensor of ISRO's Chandrayaan 1 mission, dedicated to map the surface mineral composition, provided an opportunity to map the lunar regolith in Global and Target modes. These high resolution hyperspectral data is used to recalibrate the pioneer work of [Lucey et al. \(2000\)](#) and thus estimated the FeO and TiO₂ contents of the regolith. As the FeO and TiO₂ estimations have to handle a huge amount of data, Support Vector Regression analysis (SVR) is introduced to reform the FeO and TiO₂ wt % equations for Apollo and Luna landing sites. These equations with the optimized origin are used to estimate the FeO and TiO₂ contents of the target locations. Catharina crater of the lunar near side is taken as the study area and FeO and TiO₂ wt% of the crater are estimated with M3 data. Composite chemical content (FeO wt%+ TiO₂ wt %) of the Catharina crater is estimated. LRO mini RF, Hybrid-polarized, dual-frequency synthetic aperture radar of LRO mission is used to characterize the back scattering properties of the crater surface. Stokes parameters are extracted from the LRO mini RF SAR data for the same study area. Composite chemical content estimated using M3 data is compared with the Stokes total intensity parameter extracted from the LRO mini RF data. The total intensity parameter (Stokes vector S1) is directly proportional to the composite chemical content and thus shows a linear relationship.

1. Introduction

Optical, multispectral, hyperspectral, Microwave, Lidar, etc., the familiar remote sensing techniques have their own importance in planetary studies and are capable of providing vital information about the evolution of the universe, planets, satellites, etc. The extra terrestrial explorations begin from the nearest celestial body to the earth and hence moon is considered as the origin for such explorations. So the selenological evolution of the lunar regolith is a vital factor and it should be analysed in detail. Chemical contents of the regolith can provide information about the factors and selenological processes that lead to the formation of the lunar regolith. Chemical analysis of the lunar returned samples of Apollo and Luna missions revealed the mineral composition of the regolith precisely. This laboratory analysis confirmed that Ferrous Iron and Titanium as the major transition elements governs the physical and chemical properties of the regolith. Hence the estimation of Iron and Titanium bearing minerals has significance, in understanding the formation and evolution of the lunar regolith. Thickness of the debris made regolith is different in high lands and Mare regions. The thickness of the regolith is more in High lands and it varies from 14- 15 meters, compared to the thickness of the Mare region which varies from 4-5 metres ([Murty et al., 2015](#); [McKay et al., 1991](#)). Several attempts have been made to study and understand the chemical contents of the lunar regolith for last 3-4 decades. Each of such attempts strengthens the scientific society through their valuable contributions.

[Kumar and Kumar \(2024\)](#) carried out the successful recalibration of the pioneer work of [Lucey et al. \(2000\)](#). They estimated the Optical Maturity Parameter as well as the FeO and TiO₂ contents of the lunar near side craters with hyperspectral data captured by Moon Mineralogy Mapper (M3). Linear and nonlinear data fitting techniques are used for the estimation purpose. Due to the larger complexities of lunar data sets,

computational problems aroused and so the techniques have to be modified to handle big data sets and nonlinear complexities. Machine learning based support vector regression (SVR) is introduced for data fitting by [Kumar et al. \(2025\)](#) and the estimated results are compared with the SAR images of the target locations.

2. Materials and study area

The Moon Mineralogy Mapper (M3), one of the Hyperspectral sensors of Chandrayaan-1 Mission captured lunar images in Global as well as target modes. The M3 Global data and SAR data from Mini-RF sensor of Lunar Reconnaissance Orbiter (LRO) are the prime geospatial data used for the current research. The standard Chemical contents of Ferrous oxide and Titanium dioxide of the lunar landing sites are also used for these estimations.

Both of the satellite data sets are freely available in JPL Planetary Data System (PDS) imaging node. The M3 reflectance data (NASA level 2) and LOC data (NASA level 1B) have been used in the current work ([Boardman et al., 2011](#); [Lundeen et al., 2011](#)). The level 2 reflectance data is Seleno referenced using the LOC data and is used for the analysis purpose. The Seleno referenced Reflectance data of the Apollo and Luna landing sites is used as training data, while that of the lunar near side Catharina crater is used as testing data. In the Global and target modes of data acquisition, the sensor captures lunar images from the orbits of 200 km and 100km respectively. Target and global modes have a spatial resolution of 70m/pixel and 140m/pix respectively. The Spectral resolution of the target mode is 10 nm and that of Global mode is 20nm or 40 nm respectively. The spectral range of M3 for data acquisition is from 430nm to 3000nm region of the electromagnetic spectrum. NASA level 0, NASA level 1B and NASA level 2 are the

available data products of M3 Sensor. The level 0 data is raw data in Digital Number units, level 1 data is the radiance data and level 2 is the reflectance data respectively. Band interleaved by Line and 32 bit floating point are the image and data file formats of the M3 respectively. Average size of M3 data strip is 2.8 GB (Boardman et al., 2011; Lundeen et al., 2011).

The Mini-RF has acquired data in bistatic mode, a supporting ground station transmits, and Mini-RF receives the backscattered signal as a function of bistatic angle (Fasset et al., 2023). The back scattering properties of the crater surfaces are characterized by the mini RF SAR. This instrument operates at S- (12.6 cm) and X/C-band (4.2 cm) of the electromagnetic spectrum and hence a dual-frequency Synthetic Aperture Radar (SAR). It comes under the category of Hybrid-polarized SAR. The two modes of data acquisition of Mini- RF are known as burst mode and continuous mode. The Burst mode product is the standard SAR product and continuous mode product is the interferometry application products (Reid et al., 2010).

An impact basin located in the near side of the lunar surface with significant geomorphological characteristics is selected as the study area. It should be easily located from the satellite data based on its geomorphological characteristics. For the current study we have selected Catharina crater located in the southern highlands with central coordinates of 18.00°S and 23.60°E as the target location.

3. Method of Estimation

Lucey et al. (2000) mapped and estimated lunar surface's FeO and TiO₂ Chemical contents quantitatively by making use of Clementine multispectral data and standard chemical contents of lunar landing sites in accordance with the USGS spectral library. Kumar and Kumar (2014, 2024) repeatedly recalibrated this work with hyperspectral data from Moon Mineralogy Mapper and estimated the lunar chemical contents qualitatively as well as quantitatively. Support Vector Regression analysis (SVR) is introduced by Kumar et al. (2025) to enhance the existing FeO and TiO₂ estimation techniques. Murty et al. (2015) modelled the FeO +TiO₂ vertical variations with the regolith thickness. The present scenario tries to study the variations of FeO +TiO₂ weight percentages of lunar regolith with the total intensity of the received electromagnetic field (Stokes parameter S1) of the Mini-RF SAR data. The current research is based on an assumption that the lunar regolith maturation is an ultimate slow process and hence the temporal variations of two different data sets (M3 Hyperspectral data and Mini RF SAR data), are comparatively negligible. The Flow diagram of chemical contents estimation is given in Figure 1

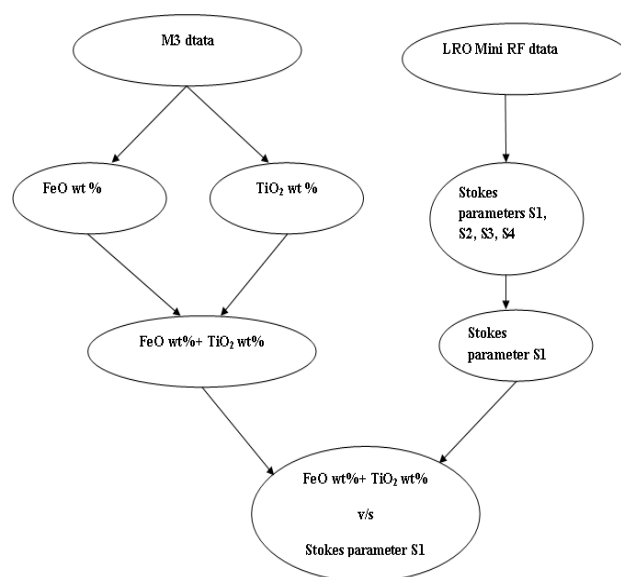


Figure. 1: Flow diagram of Chemical Contents estimation

To execute the current research initially, desired M3 data is downloaded from the NASA JPL PDS imaging node followed by data preprocessing has to be done. In this phase spatial subsetting, geo referencing of the M3 data, desired band selection, band averaging etc. should be carried out. In the data processing phase origin optimization, Iron and Titanium inversion parameter generation for lunar landing sites, FeO and TiO₂ weight percentage equation generation etc. have been carried out (Kumar and Kumar 2014, 2024). This is the training phase and after that testing of the model is carried out. Iron and Titanium inversion parameters are generated for the Catharina crater the target location, and corresponding weight percentages are estimated. In the final phase or data post processing phase, required maps are generated and statistical parameters are computed (Kumar and Kumar 2014, 2024). Iron inversion parameters for M3 data is given in Eqn. 1

$$\Theta_{Fe} = -\tan^{-1} \left[\frac{\left(\frac{R_{950}}{R_{750}} - 1.18 \right)}{\left(\frac{R_{750}}{R_{750}} - 0.08 \right)} \right] \quad (1)$$

Where,

R_{750} = Spectral average around 750nm $(R_{730}+R_{750}+R_{770})/3$

R_{950} = Spectral average around 950nm $(R_{930}+R_{950}+R_{970})/3$

(0.08, 1.18) is Iron inversion spectral constants for M3 data known as optimized origin.

Similarly Titanium inversion parameters for M3 data is given in Eqn. 2

$$\Theta_{Ti} = \tan^{-1} \left[\left(\frac{R_{540}}{R_{750}} - 0.71 \right) / (R_{750} - 0.07) \right] \quad (2)$$

Where R_{540} and R_{750} are the spectral reflectance values of 540nm and 750nm respectively and (0.07, 0.71) represents the

origin or spectral constants of M3 data for TiO₂ estimation. The Spectral constants or origin values correspond to the combination of a specific sensor, Chemical element, and standard spectral library used to analyze the reflectance spectra are to be a constant (Kramer et al., 2011; Kumar and Kumar 2014, 2024; Lucey et al., 2000).

Individual chemical contents of FeO and TiO₂ of the Catharina crater are estimated according to Kumar et al. (2025). With the estimated M3 origins for FeO and TiO₂, Chemical inversion parameters of the Catharina crater for both of the estimations are generated. To estimate the chemical contents of target location, the Catharina crater, Iron and Titanium inversion parameters of the lunar landing sites in the corresponding weight percentage equations are replaced with the newly estimated chemical inversion parameters of the target location. The Support Vector Regression (SVR) analysis is used for the FeO and TiO₂ weight percentage equation generation and is implemented with Python programming.

Support Vector Machines (SVM), the big data classifier can be further extended for regression analysis. The regression problem tries to find a function that approximates mapping from an input domain to the real numbers based on systematic training (Soman et al., 2011). The SVR can be considered as a typical extension of large margin kernel methods for classification to the regression analysis. It retains all the properties that characterize maximal margin algorithms of the SVMs. The SVR is a powerful technique for predictive data analysis with the characteristics of SVM in many areas of applications. Besides the characteristic properties of SVM, the SVR formulation introduces the concept of loss function, which ignores error that lies within a distance of the true value (Soman et al., 2011).

FeO and TiO₂ weight percentage equations are given in Eqn. 3-4 respectively.

$$FeO_{wt} \% = 0.566 \times \Theta_{Fe}^2 + 11.732 \times \Theta_{Fe} - 1.592 \quad (3)$$

$$TiO_2_{wt} \% = 16.171 \times \Theta_{Ti}^2 - 31.936 \times \Theta_{Ti} + 16.061 \quad (4)$$

The Composite chemical content (FeO+ TiO₂) of the Catharina crater is estimated from the individual chemical contents.

Optical wavelengths of the electromagnetic spectrum can be focused by a lens while that of the microwave region (1mm - 1m) can be focused with an antenna. Imaging radar systems used for remote sensing purposes are pulsed types. Energy transmissions of such systems are for a very short interval of time. Transmitted pulses (energy) interact with the target and some amount of energy may be backscattered and received by the antenna (Lush 1999). A pulse repetition frequency maintains the transmission of pulses and ensures sufficient time for returning the back scatter from far objects before transmitting the next pulse (Lush 1999). As electromagnetic energy has two components ie. electric and magnetic components, the electric field component becomes oriented vertically, horizontally, or at some other angles. This orientation of the electric field is known as polarization (Lush 1999.). Orientation of the transmitted and backscattered energy can be controlled and may provide 4 different possible polarizations.

HH horizontal transmit and horizontal receive

VV vertical transmit and vertical receive

HV horizontal transmit and vertical receive

VH Vertical transmit and horizontal receive

If the radar system uses four modes of polarization, the radar is known as quadrature polarimetric or quad pol.

Stokes vector or Stokes parameters completely represent a polarized electromagnetic wave. Gabriel Stokes developed this method of representation and is enough to describe the information associated with a polarized wave and is given by Eqn. 5

$$\begin{bmatrix} S1 \\ S2 \\ S3 \\ S4 \end{bmatrix} = \begin{bmatrix} \langle |E_H|^2 + |E_V|^2 \rangle \\ \langle |E_H|^2 - |E_V|^2 \rangle \\ 2 \text{Re} \langle E_H E_V^* \rangle \\ -2 \text{Im} \langle E_H E_V^* \rangle \end{bmatrix} \quad (5)$$

Here S1, S2, S3 and S4 are the four Stokes parameters that represent total intensity, degree of polarization, phase, etc of the received electromagnetic wave (Woodhouse 2006). Such an electromagnetic wave having these four types of information represents the SAR data in the Current research. E_H and E_V represents the received horizontal and vertical components of the electric field vector respectively. Re and Im represents the real and imaginary parts of the electric field vector. < > represents ensemble averaging.

The Mini RF Transmits right circular polarized signals only. But it simultaneously receives Horizontal polarized signals as well as vertical polarized signals and the phase between the two polarizations. A level 2 unit pixel data of MiniRF sensor bears 4 types of information that can be represented by 4 Stokes parameters. The first Stokes parameter S1 represents the total power or total intensity of the received field or additive property. The Second Stokes parameter S2 represents the subtractive property or the difference between the horizontal and vertical components of polarization of the received electromagnetic field. This component discriminates the type of polarization either vertical or horizontal. The third and fourth Stokes parameters represent the cosine and sine components of the average phase between the horizontally and vertically polarized components of the received field respectively (Reid et al 2010). The third parameter S3 represents the wave nature, ie. linear, elliptical or circular. Fourth component S4 provides the information of rotation or handedness (either left handed or right handed). Out of the 4 Stokes parameters S2, S3 and S4 are independent parameters, while S1, the total intensity parameter depends on the other three Stokes parameters.

The Stokes parameters are extracted from the LRO Mini-RF data. The total intensity component of SAR data or First Stoke parameter (S1) is plotted against the composite chemical content.

The entire process is completed in two phases Hyperspectral phase or simply M3 phase and SAR phase. In the M3 phase, initially, data pre processing has to be completed, followed by data processing, which comprises training of the model and testing of the target location. Finally, data post processing, map generation, and statistical parameter computation etc. have been completed. In the SAR phase, Stokes parameters are computed.

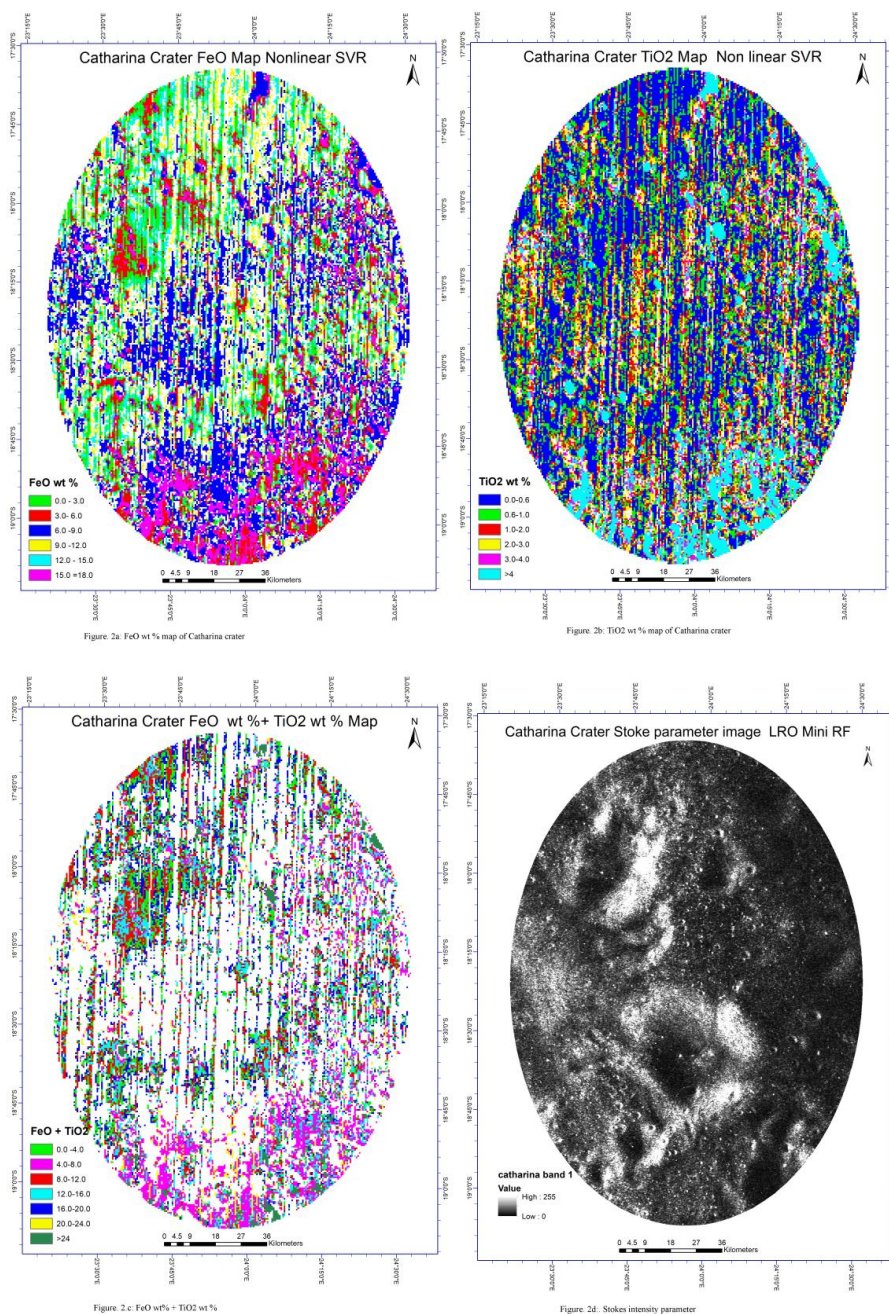
Composite Chemical content extracted in M3 phase is plotted against the total intensity or first Stoke parameter S1 of the Mini-RF SAR data extracted in the SAR Phase.

4. Results

With the standard origins of M3 data for FeO and TiO₂ estimations, Iron and Titanium inversion parameters are generated for the Apollo and Luna landing sites using the SVR analysis. Then the FeO and TiO₂ contents of the Catharina crater are estimated separately. The Composite chemical content of the Catharina crater is derived from the individual chemical contents of FeO and TiO₂.

The FeO wt % of the Catharina crater varies from 0.0213-18.2329. Average FeO wt% is 9.34. The TiO₂ wt% varies from 0.2934-13.987. Average TiO₂ wt% is 2.56. Figures 2a and 2b represent the FeO and TiO₂ contents of the Catharina crater. The Composite Chemical content, FeO wt % + TiO₂ wt% of the Catharina crater is calculated and is represented in Figure 2c. Stokes total intensity parameter is computed from LRO Mini-RF data and is given in Figure 2d.

The plot between FeO wt% + TiO₂ wt% and Stokes first parameter of total intensity, results with a straight line and establishes a linear relationship between them. The composite chemical content v/s total intensity plot is given in Figure 3.



Chemical contents and stoke parameter maps of Catharina crater

This contribution has been peer-reviewed.

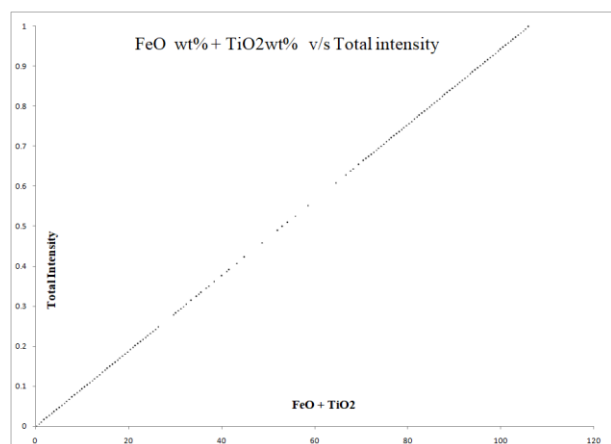


Figure.2: Composite chemical content v/s total intensity (Stokes parameter S1)

5. Discussion conclusions and feature work

The FeO and TiO₂ weight percentages of the Catharina crater are estimated separately and the composite chemical content of the crater is derived from these individual weight percentages and analyzed with the Stokes total intensity parameter. The FeO and TiO₂ contents are estimated from M3 hyperspectral data through SVR analysis between chemical inversion parameters and standard chemical contents of the lunar landing sites. NASA level 2 reflectance images of M3 provided spectral reflectances around 540nm, 750nm, and 950nm regions of the electromagnetic spectrum for those estimations. The Stokes parameter S1 represents the total intensity of the received polarized electromagnetic wave (SAR data). Basically, reflectance energy was recorded by two different advanced remote sensing techniques and both of the outcomes show a linear relationship and hence complementary to each other. There is a linear relationship between Composite chemical content and the total intensity of the received field of the lunar regolith subject to the sensor parameters, spectral library and chemical inversion parameters. To establish this relation we require the hyperspectral, SAR data and standard chemical contents of the lunar landing sites as well as the target locations. Unfortunately, due to the lack of required data it can be established in feature subject to the availability of necessary data. As regolith is the major repository of the information retrieved from moon, it is essential to estimate its thickness and chemical composition of the regolith in a feature work. The low dielectric constant value and desiccated nature of the regolith allows microwave signals to penetrate into it. So the Lunar regolith thickness should be estimated from SAR data. The M3 based chemical content estimation, mainly provides the lateral variations of FeO and TiO₂ along the lunar regolith while the vertical variation of FeO and TiO₂ wt% should be estimated from SAR data. Murty et al. (2015) proposed a modelling technique with SAR data for the same. It can be implemented with the SVR wt% equations for FeO and TiO₂ along with Suitable SAR data.

6. References

Boardman, J.W., Pieters, C.M., Green, R.O., Lundeen, S.R., Varanasi, P., Nettles, J., Petro, N., Isaacson, P., Besse, S., Taylor, L.A., 2011: Measuring moonlight: An overview of the spatial properties, lunar coverage, selenolocation, and related Level 1B products of the Moon Mineralo-

gy Mapper. Journal of Geophysical Research, Planets 116. <https://doi.org/10.1029/2010JE003730>.

Fasset, C.I., Patterson, G., Valentin, E. R., Stickle, A., Morgan, G., 2023: LRO Mini-RF Bistatic Observations of Cabeus Crater Revisited. Bulletin of the AAS, LPSC 54, Vol. 55, Issue 8 abs. no. 1564.

Kramer, G.Y., Besse, S., Nettles, J., Combe, J. P., Clark, R.N., Pieters, C.M., Staid, M., Malaret, E., Boardman, J., Green, R.O., 2011: Newer views of the Moon: Comparing spectra from Clementine and the Moon Mineralogy Mapper. Journal of Geophysical Research, VOL. 116, E00G04. <https://doi.org/10.1029/2010JE003728>.

Kumar, P.A., and Kumar, S., 2014: Estimation of optical maturity parameter for lunar soil characterization using Moon Mineralogy Mapper (M3). Advances in Space Research, Vol. 53, Issue 12, 1694–1719. <https://doi.org/10.1016/j.asr.2014.01.009>

Kumar, P.A., and Kumar, S., 2024: A spectrophotometric evaluation of lunar nearside craters Catharina and Cyrillus for estimations of FeO, Optical maturity and TiO₂. Advances in Space Research, Vol. 73, Issue 4, 2203–2231. <https://doi.org/10.1016/j.asr.2023.07.050>.

Kumar, P.A., Kumar, S., Advait, C.A., 2025: A Spectrophotometric evaluation of Lunar Catharina crater using support vector regression analysis for FeO and TiO₂ estimations, Accepted to ISPRS Geospatial week 2025, Dubai .

Lucey, P.G., Blewett, D.T., Jolliff, B.L., 2000: Lunar Iron and Titanium abundance algorithms based on final processing of Clementine ultraviolet-visible images. Journal of Geophysical Research, Planets, Vol. 105, 20297–20305. <https://doi.org/10.1029/1999JE001117>.

Lusch D. P., 1999: Introduction to microwave Remote sensing, Centre for Remote Sensing and Geoinformation Science, Michigan State University

Lundeen, S., McLaughlin, S., Alanis, R., 2011: Moon Mineralogy Mapper (M3) Moon Mineralogy Mapper Archive volume Software Interface Specification.

McKay, D., Heiken, G., Basu, A., Blanford, G., Simon, S., Reedy, R., French, B., Papike, J., 1991: The lunar regolith in Heiken, G.H Vaniman, D.T., French, B.M. (Eds.) Lunar Source-book. Cambridge Univ. press, New York, pp. 285–356.

Murty, S. V. S., Vijayan, S., Mohan, S., 2015: Lunar regolith thickness estimation using dual frequency microwave brightness temperature and influence of vertical variation of FeO + TiO₂, Planetary and space science, Vol. 105, 123–132. <https://doi.org/10.1016/j.pss.2014.11.017>.

Reid, M., La Valle, D. B., Winters, H., Bussey, D. B., Slavney, S., Acton, C., 2010: PDS data Product Software Interface Specification (SIS) for Mini-RF advanced technologies – Lunar Reconnaissance Orbiter (LRO) payload operations center, specification number: MRF-4009, cage code 12934, JPL, NASA.

Soman, K. P., Loganathan, R., Ajay, V., 2011: Machine Learning with SVM and Other Kernel Methods, PHI Learning Private Ltd New Delhi.

Woodhouse, I.H., 2006: Introduction to Microwave remote sensing, Taylor and Francis, Boca Raton, Florida, USA.
<https://doi.org/10.1201/9781315272573>